N-cadherin mediates plasticity-induced long-term spine stabilization

Pablo Mendez, Mathias De Roo, Lorenzo Poglia, Paul Klauser, and Dominique Muller

Department of Neuroscience, University of Geneva, Faculty of Medicine, 1211 Geneva, Switzerland

Excitatory synapses on dendritic spines are dynamic structures whose stability can vary from hours to years. However, the molecular mechanisms regulating spine persistence remain essentially unknown. In this study, we combined repetitive imaging and a gain and loss of function approach to test the role of N-cadherin (NCad) on spine stability. Expression of mutant but not wild-type NCad promotes spine turnover and formation of immature spines and interferes with the stabilization of new spines. Similarly, the long-term stability of preexisting spines is reduced when mutant NCad is expressed but enhanced in spines expressing NCad-EGFP clusters. Activity and long-term potentiation (LTP) induction selectively promote formation of NCad clusters in stimulated spines. Although activity-mediated expression of NCad-EGFP switches synapses to a highly stable state, expression of mutant NCad or short hairpin RNA–mediated knockdown of NCad prevents LTP-induced long-term stabilization of synapses. These results identify NCad as a key molecular component regulating long-term synapse persistence.

Introduction

Spine formation and elimination proceeds at a very high rate during development of cortical networks (Lendvai et al., 2000; Holtmaat et al., 2005; Zuo et al., 2005). Under these conditions, a great proportion of newly formed protrusions is only transient and disappears within days after formation (De Roo et al., 2008a). However, others are more persistent and may remain for weeks or even months (Grutzendler et al., 2002; Trachtenberg et al., 2002). Although the molecular mechanisms regulating the long-term behavior of spines remain essentially unknown, several studies have proposed that spine size and activity could represent important factors (for review see Kasai et al., 2003). Spine head size correlates with stability in both in vivo and in vitro studies (Holtmaat et al., 2005; De Roo et al., 2008a), and long-term potentiation (LTP) is associated with a rapid enlargement of the spine head that persists for hours (Matsuzaki et al., 2004; Harvey and Svoboda, 2007; Kopec et al., 2007). This enlargement correlates with a remodeling of the postsynaptic density (PSD), an increased expression of AMPA receptors (Matsuzaki et al., 2004; Zito et al., 2009), and a reorganization of the actin cytoskeleton (Honkura et al., 2008). It depends on protein synthesis and neurotrophin signaling (Tanaka et al., 2008) and involves increased dynamics of PSD proteins such as PSD-95 and Shank-1 (Steiner et al., 2008). These changes are thus directly related to the increase in synaptic strength but could also be part of a process that provides a better stability to the spine. In recent work, we found that LTP induction is indeed able to switch potentiated spines to a highly stable state, making these spines persistent for several days (De Roo et al., 2008b). This process is selective because nonstimulated spines conversely became destabilized and tended to be eliminated and replaced by new ones. Together, these results support the idea that synaptic plasticity not only regulates synaptic strength but also contributes to the long-term maintenance of spine synapse.

How this is achieved remains unclear. The process could be nonselective and simply related to the number of receptors and/or PSD molecules accumulated at the synapse. Thus, stability would vary according to the continuous fluctuations of spine size (De Roo et al., 2008b; Yasumatsu et al., 2008). However, it could be also that stability depends on expression of a specific set of synaptic proteins, which would in this way tag potentiated synapses as recently shown for Homer-1a (Okada et al., 2009).

Correspondence to Dominique Muller: Dominique.Muller@unige.ch

P. Mendez's present address is European Brain Research Institute, Roma 00143, Italy.

Abbreviations used in this paper: ANOVA, analysis of variance; LTP, long-term potentiation; mRFP, monomeric RFP; NCad, N-cadherin; NMDA, *N*-methyl-D-aspartic acid; PSD, postsynaptic density; shRNA, short hairpin RNA; WT, wild type.

The Rockefeller University Press $30.00
J. Cell Biol. Vol. 189 No. 3 589–600
www.jcb.org/cgi/doi/10.1083/jcb.201003007

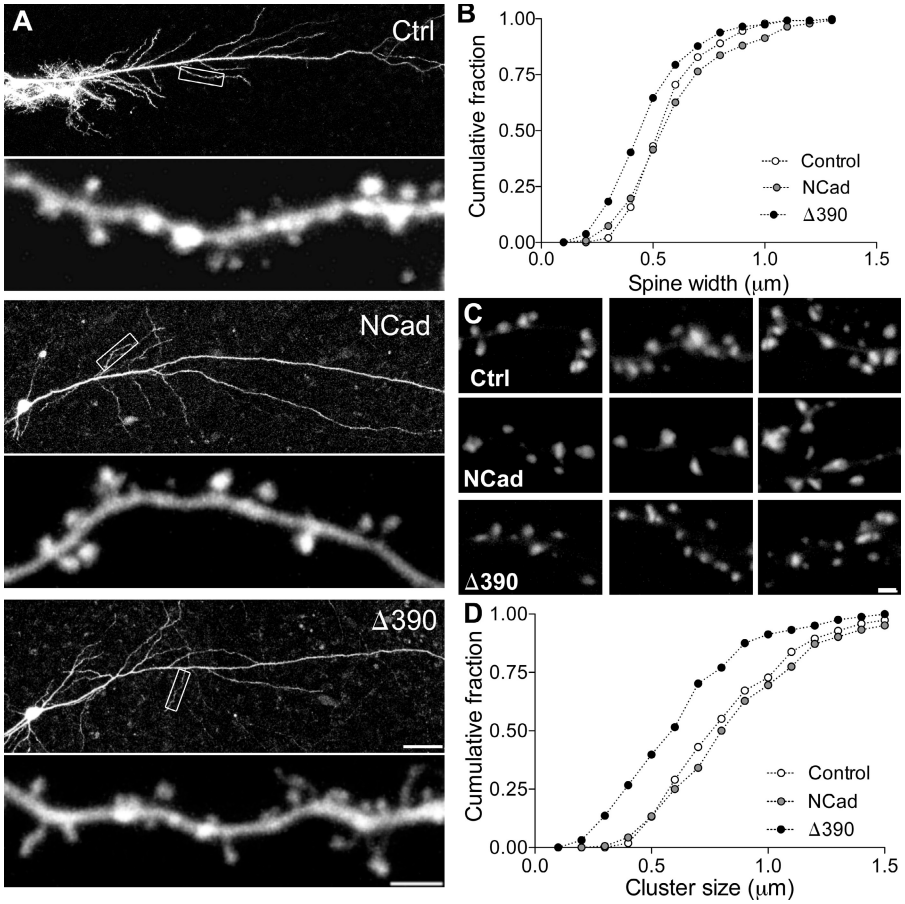

Figure 1. **NCad regulates spine morphology and PSD size.** (A) Dendritic segments from pyramidal CA1 neurons transfected with EGFP (Ctrl), EGFP + WT-NCad (NCad), or EGFP + the mutant Δ390-NCad (Δ390). Note the increased proportion of thin, immature-type spines in the cell transfected with Δ390-NCad. Boxes show the corresponding enlarged dendritic segments below. (B) Cumulative distribution of spine head width in the three conditions, indicating a shift to the left in Δ390-NCad cells ($n = 5$; $P < 0.001$; one-way ANOVA). (C) PSD-95–EGFP puncta in cells transfected with PSD-95–EGFP (Ctrl), PSD-95–EGFP + NCad (NCad), or PSD-95–EGFP + Δ390-NCad (Δ390). (D) Cumulative distribution of the size of PSD-95–EGFP puncta in the three conditions. Note the shift to the left in Δ390-NCad–transfected cells ($n = 4$; $P < 0.001$; one-way ANOVA). Bars: (A, top) 50 μm; (A, bottom) 2 μm; (C) 1 μm.

Among candidate molecules for providing stability, adhesion molecules are of particular interest and could play such a role through their adhesive and recognition properties. In this study, we investigated this possibility focusing on N-cadherin (NCad), one of the most important adhesion molecules for synapse formation and plasticity (Arikkath and Reichardt, 2008). NCad function regulates spine morphology (Togashi et al., 2002; Abe et al., 2004; Okamura et al., 2004; Elia et al., 2006; Xie et al., 2008; Arikkath et al., 2009) and is required for the late-phase LTP (Tang et al., 1998; Okuda et al., 2007). Its interaction with AMPA receptors affects spine density (Saglietti et al., 2007), and its surface expression is modulated by *N*-methyl-D-aspartic acid (NMDA) receptors (Tai et al., 2007). Thus, NCad could exert a major role in plasticity-induced stability. We examined in this study this possibility using a repetitive imaging approach that allowed us for the first time to assess spine stability over days in relationship to NCad expression and plasticity. The results provide strong evidence that NCad is indeed critically related to spine stability and that its expression is required for the long-term persistence of potentiated synapses.

Results

Cadherin regulates spine and PSD size and morphology

To investigate the function of NCad in activity-dependent plasticity, we used a biolistic approach to transfect CA1 cells from organotypic hippocampal slice cultures with constructs expressing EGFP as control, wild-type (WT) NCad (WT-NCad), the mutant Δ390-NCad, or tagged versions of WT-NCad (NCad-EGFP). The Δ390-NCad mutant is characterized by a deletion of the extracellular domain that renders it nonfunctional for intercellular adhesion and interaction. It also competes with endogenous NCad for intracellular signaling, thus exerting a dominant-negative effect, inhibiting the multiple types of classical cadherins expressed in the hippocampus (i.e., NCad, cadherin-8, and cadherin-11; Togashi et al., 2002). We transfected neurons at day 11 in vitro and, after 2–3 d, imaged them repetitively on several consecutive days, and analyzed the dynamics and morphology of spines on identified segments of secondary or tertiary dendrites. In agreement with previous observations (Togashi et al., 2002), we found, as shown in Fig. 1, that spines on neurons transfected with the mutant Δ390-NCad exhibited an altered morphology and, in particular, features of immaturity: spines were characterized by smaller heads than in control or WT-NCad–expressing neurons, and the proportion of filopodia-like structures (protrusions without enlargement at the tip) were more frequent in mutant Δ390-NCad–transfected cells than in control or WT-NCad–transfected neurons (control, 5.3 ± 0.8%; WT-NCad, 5.4 ± 1.7%; Δ390-NCad, 14.2 ± 2.3%; Fig. S1). Fig. 1 B shows the size distribution of spine head measurements under the three conditions, revealing a significant shift to the left of spine heads values in Δ390-NCad mutant cells (mean head width: 0.60 ± 0.01 μm, 0.64 ± 0.02 μm, and 0.52 ± 0.01 μm in EGFP [control]-,

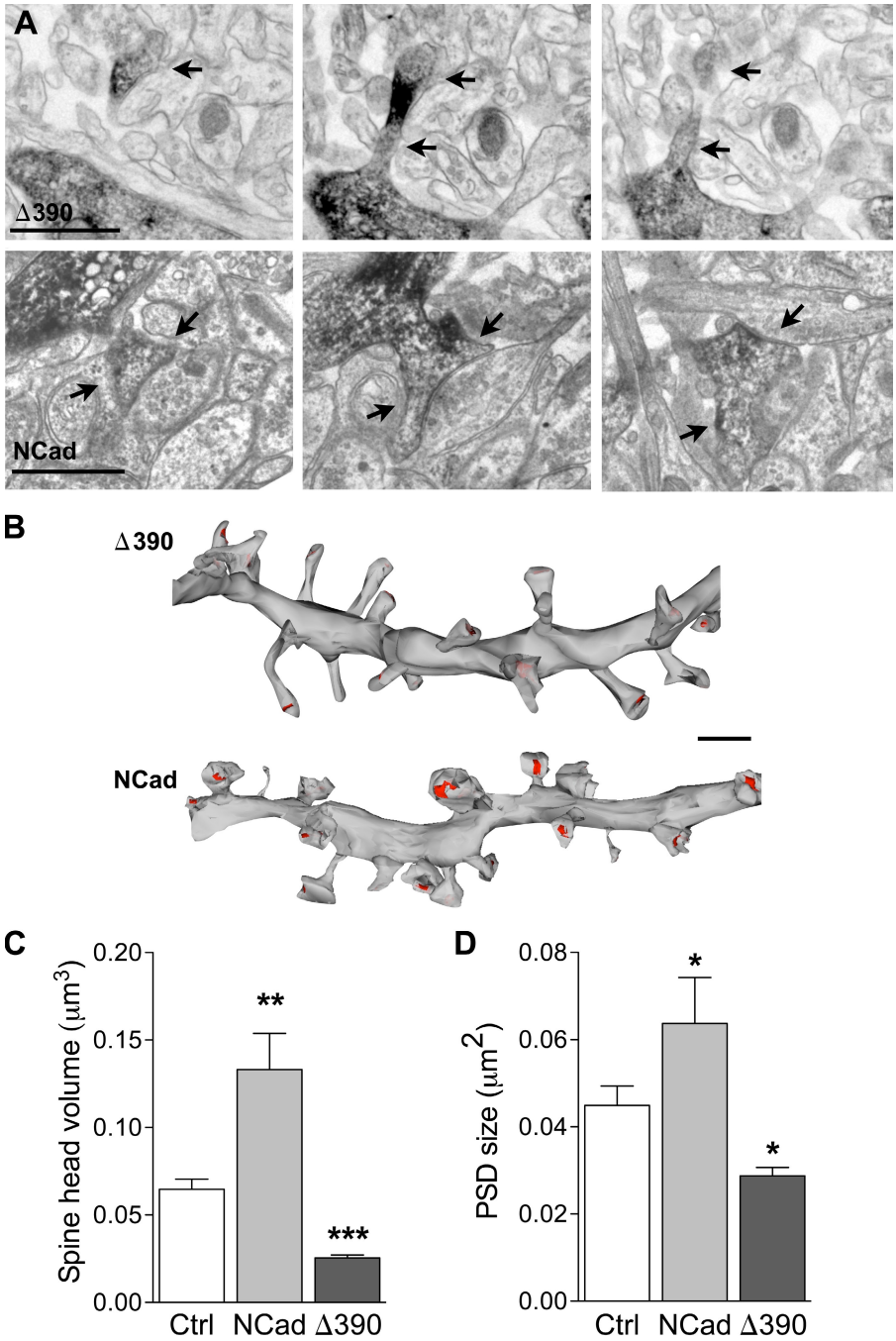

Figure 2. **Regulation of spine ultrastructure by NCad.** (A) Illustrations of dendritic spines (arrows) visualized on consecutive sections obtained from a dendritic segment of a pyramidal CA1 neuron transfected with EGFP + Δ390-NCad (Δ390) or EGFP + NCad (NCad). The transfected dendritic segment is revealed by anti-EGFP immunostaining. (B) 3D reconstruction of two dendritic segments obtained from cells transfected with EGFP + Δ390-NCad or EGFP + NCad. Note the differences in size of spine heads and PSD areas (red). (C and D) Quantitative analysis of spine head volume and PSD area obtained from 3D-reconstructed dendritic segments of CA1 pyramidal neurons transfected with EGFP (Ctrl), EGFP + NCad, or EGFP + Δ390-NCad. Data are mean ± SEM of three experiments per condition (110, 58, and 127 reconstructed spines analyzed; *, $P < 0.05$; **, $P < 0.01$; ***, $P < 0.001$; Mann-Whitney *U* test). Bars: (A) 1 μm; (B) 2 μm.

WT-NCad–, and mutant Δ390-NCad–transfected cells, respectively; $P < 0.01$). The mean length of protrusions was not significantly different between groups (mean spine length: 1.09 ± 0.04 μm, 1.12 ± 0.03 μm, and 1.19 ± 0.03 μm for EGFP, NCad, and Δ390-NCad groups, respectively; $P > 0.1$). However, there were small differences in spine density, which tended to be smaller in WT-NCad–transfected cells (0.84 ± 0.03 μm^{-1} in control EGFP-transfected cells vs. 0.76 ± 0.05 μm^{-1} in Δ390-NCad and 0.65 ± 0.03 μm^{-1} in WT-NCad–transfected neurons).

We then investigated whether altered spines in Δ390-NCad–expressing neurons formed synapses, and for this, we analyzed PSDs visualized through PSD-95–EGFP expression in transfected cells and also through electron microscopic 3D reconstruction of dendritic segments. As illustrated in Fig. 1 C, PSD-95 puncta could clearly be identified in dendrites of all transfected cells, but their size was significantly reduced in Δ390-NCad–expressing cells as compared with WT-NCad– or EGFP-transfected neurons (0.65 ± 0.02 μm vs. 0.91 ± 0.02 μm and 0.86 ± 0.02 μm, respectively; $n = 161–265$; $P < 0.001$, one-way analysis of variance [ANOVA]). This was further confirmed by EM analyses of serial sections obtained from transfected neurons. Fig. 2 A shows illustrations of consecutive sections of small dendritic segments with their attached spines (arrows), as revealed by EGFP antibodies. Fig. 2 B shows the 3D reconstruction of two segments obtained one from a Δ390-NCad– and the other from an NCad-transfected neuron. As illustrated,

spines of mutant Δ390-NCad–transfected neurons were smaller in size, showed more irregular shapes with many more thin spines resembling filopodia-like protrusions, and they were also characterized by a significant decrease in the size of their PSDs, indicated in red on the figure (Fig. 2 B). However, most spines, although immature in morphology, were engaged in synaptic contacts with a presynaptic partner. Interestingly, expression of WT-NCad also affected spine morphology. As indicated in the quantitative analyses of Fig. 2 (C and D), the size of the spine heads was significantly increased in comparison with EGFP-transfected neurons, as well as PSDs, although to a smaller extent (n = 110, 58, and 127 reconstructed spines in EGFP [control]-, NCad-, and Δ390-NCad–transfected neurons, respectively; *, $P < 0.05$; Mann-Whitney U test). Together, these results indicated that NCad function is not required for synapse formation but is involved in the development of the spine head and facilitates the expression of PSD-95 on new spines.

NCad loss of function results in increased spine turnover

As a defect of spine maturation could affect spine dynamics, we then measured spine turnover and stability on several consecutive days. We quantified these changes by analyzing dendritic segments obtained from 23 EGFP-, 9 WT-NCad–, and 9 Δ390-NCad–transfected cells, measuring the behavior of a total of 1,166, 449, and 523 spines, respectively, over 48 h. Fig. 3 A shows illustrations of dendritic segments from NCad- and Δ390-NCad–transfected neurons and imaged at 24-h intervals. The data, summarized in Fig. 3 B, indicate that the number of newly formed and lost spines detected over periods of 24 h were significantly increased in the Δ390-NCad group, but, conversely, new spines were less numerous after WT-NCad transfection. Overall, the turnover rate, calculated as half the sum of new and lost protrusions per 24 h and expressed as the percentage of the number of initial spines (De Roo et al., 2008a), increased from 20 ± 1% in EGFP control cells to 43 ± 5% in the Δ390-NCad group ($P < 0.01$), whereas it decreased to 14 ± 2% in WT-NCad–expressing cells. As a result, expression of mutant Δ390-NCad led to a marked decrease in the proportion of stable spines (80 ± 1% vs. 69 ± 3%; n = 23 and 9; EGFP and Δ390, respectively; $P < 0.01$), whereas, conversely, NCad expression promoted stability. Despite these important differences in turnover rate, the spine density did not vary significantly over time between the three conditions (Fig. 3 C). Together, these experiments strongly suggested a role of NCad in regulating spine stability.

NCad loss of function interferes with new spine stabilization and PSD-95 expression

We then directly assessed spine stability by analyzing the probability that a newly formed spine would become stable with time under the three conditions tested. For this, we identified new spines formed during an interval of 5 h in five different experiments per condition and measured the proportion of them still present 24 and 48 h later. As shown in Fig. 4 A, many newly formed spines in EGFP-transfected cells were transient, and only a small fraction of them became stabilized over 2 d. However, these values

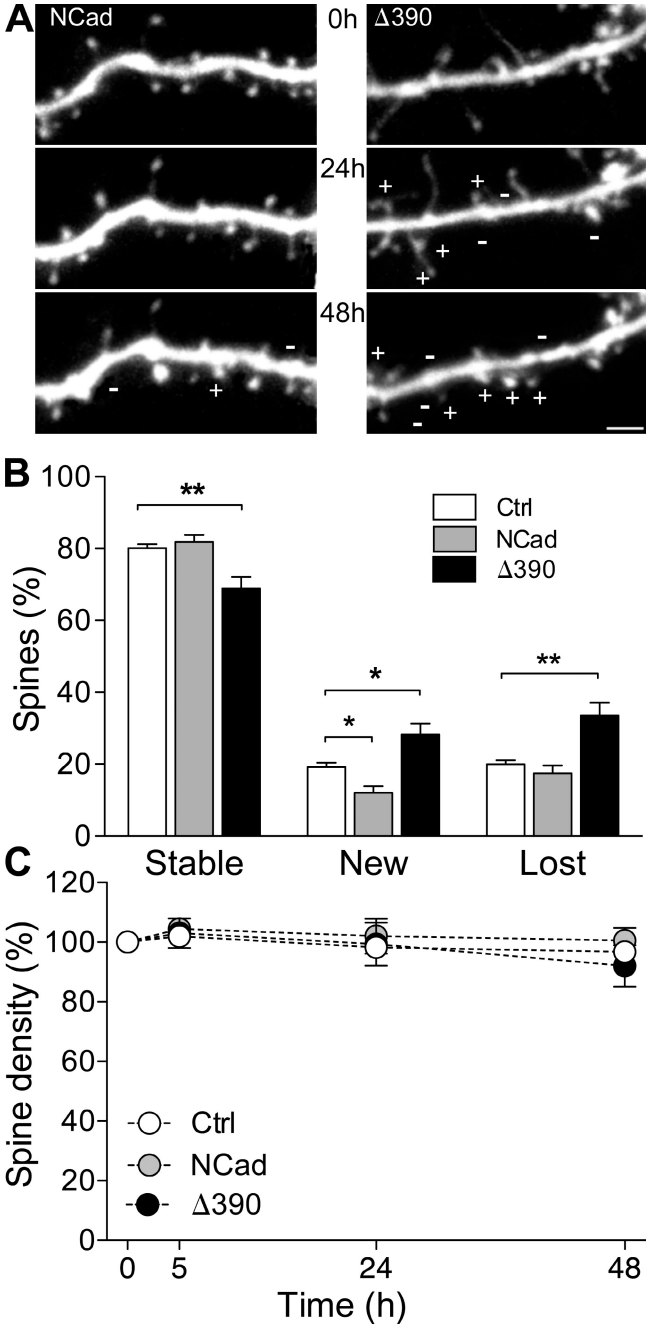

Figure 3. **Modification of spine turnover by interference with NCad function.** (A) Illustration of dendritic segments imaged repetitively at 24-h intervals and obtained from an EGFP + NCad (NCad)– and an EGFP + Δ390-NCad (Δ390)–transfected cell. Plus and minus signs indicated newly formed or lost spines, respectively. (B) Fraction of stable, newly formed, and lost spines detected over periods of 24 h in EGFP (Ctrl)-, EGFP + NCad–, or EGFP + Δ390-NCad–transfected cells. Data are mean ± SEM of 9–23 experiments (1,166, 449, and 523 spines analyzed, respectively; *, $P < 0.05$; **, $P < 0.01$; two-way ANOVA with Bonferroni posttest). (C) Changes in spine turnover are not associated with modifications of spine density in the three conditions tested. Data are mean ± SEM of 9–23 experiments. Bar, 2 µm.

were significantly reduced when expressing mutant Δ390-NCad and conversely increased with WT-NCad (n = 5; 23, 15, and 50 new spines analyzed in control, NCad, and Δ390-NCad conditions, respectively; $P < 0.05$; two-way ANOVA). Thus, NCad directly affected the stabilization of newly formed spines.

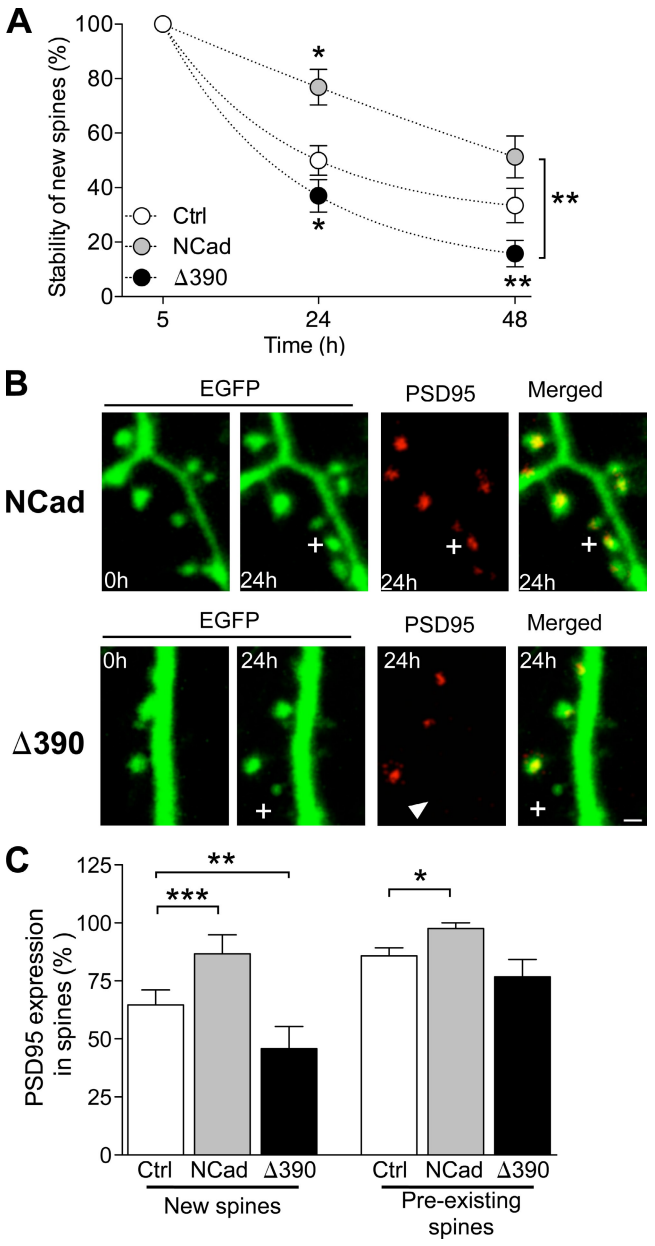

Figure 4. **NCad regulates the long-term stabilization of newly formed spines.** (A) Stability over the next 2 d of new spines formed during an interval of 5 h in EGFP (Ctrl)-, EGFP + NCad (NCad)–, and EGFP + Δ390-NCad (Δ390)–transfected cells. Data are mean ± SEM of the proportion of spines still present at the indicated times (n = 5–16; 23, 15, and 50 new spines analyzed; *, P < 0.05; **, P < 0.01; two-way ANOVA with Bonferroni posttest). (B) Expression of DsRed2-tagged PSD-95 in newly formed spines (plus signs) observed in EGFP + NCad– or EGFP + Δ390-NCad–transfected neurons. Note that the new spine illustrated in the NCad condition expresses a DsRed2–PSD-95 puncta, but not the one in Δ390-NCad (arrowhead). (C) Fraction of new spines formed in an interval of 24 h (new spines) and of spines older than 24 h (preexisting spines) that expressed DsRed2–PSD-95 puncta in the three conditions tested. Data are mean ± SEM of 4–5 experiments (26, 13, and 19 new spines analyzed and 140, 82, and 75 stable spines analyzed in five control, four NCad, and five Δ390-NCad experiments, respectively; *, P < 0.05; **, P < 0.01; ***, P < 0.001; two-way ANOVA with Bonferroni posttest). Bar, 1 µm.

Formation and stabilization of new spines is also regulated by activity. In particular, we found that blockade of AMPA receptors with 2 µM NBQX promoted a marked increase in the probability that newly formed spines will become stabilized, mimicking in this way the effect of WT-NCad expression. Therefore, we investigated whether this effect could depend on NCad function by analyzing the effect of NBQX in Δ390-NCad–transfected cells. As shown in Fig. S2, expression of mutant Δ390-NCad fully prevented the stabilizing effect of NBQX treatment, further emphasizing the role of NCad in regulating the stabilization of newly formed spines.

Finally, as expression of PSD-95 is also an important parameter affecting new spine stabilization (De Roo et al., 2008a), we examined whether interferences with NCad function could affect PSD-95 expression. For this, we cotransfected CA1 neurons with PSD-95–DsRed2 together with EGFP, EGFP + Δ390-NCad, or EGFP + WT-NCad. 2 d after transfection, we analyzed newly formed spines detected within a period of 24 h and determined the proportion of them that expressed PSD-95–DsRed2. For comparison, we also analyzed preexisting spines present from the beginning of the experiments and thus older than 24 h. Fig. 4 B illustrates two experiments, one performed with WT-NCad and the other with mutant Δ390-NCad transfection. As illustrated, the new spine formed in the Δ390-NCad–transfected cell failed to express detectable PSD-95–DsRed2 puncta. Analysis in four to five different cells per condition of the probability to express PSD-95–DsRed2 in new and preexisting spines indicated that expression of mutant Δ390-NCad significantly reduced, whereas, conversely, WT-NCad enhanced expression of PSD-95–DsRed2 in newly formed spines (n = 5 and 4; P < 0.02; two-way ANOVA; Fig. 4 C). Thus, NCad contributed to the stabilization of newly formed synapses by regulating PSD-95 expression.

NCad expression correlates with long-term spine stability

We then investigated whether NCad also affected the stability of spines already present in the tissue. For this, we transfected CA1 pyramidal cells and assessed the stability of preexisting spines by measuring the proportion of initial spines still present on consecutive days. As illustrated in Fig. 5 A, this proportion was markedly reduced in cells transfected with the mutant Δ390-NCad as compared with control EGFP- or WT-NCad–transfected cells (n = 17, 11, and 9; 547, 349, and 358 spines analyzed, respectively; *, P < 0.05; **, P < 0.01; ***, P < 0.001; two-way ANOVA). Thus, interfering with NCad function markedly reduced the long-term persistence of spines.

To examine this further, we then directly analyzed the stability of spines as a function of NCad expression. For this, we cotransfected CA1 neurons with WT-NCad–EGFP and monomeric RFP (mRFP) to visualize dendritic spines. As shown in Fig. 5 B, NCad-EGFP showed a punctuate aspect that clearly colocalized with spine heads (arrows), although not all spines expressed NCad-EGFP puncta (arrowheads). As spine stability correlated with spine head size, we then examined whether NCad-EGFP puncta were also more frequent in larger spines. As shown in Fig. 5 C, the proportion of spines expressing NCad-EGFP was directly related to the size of the spine head (n = 6; 125 spines analyzed). We then also directly assessed the stability of identified spines that did or did not express NCad-EGFP

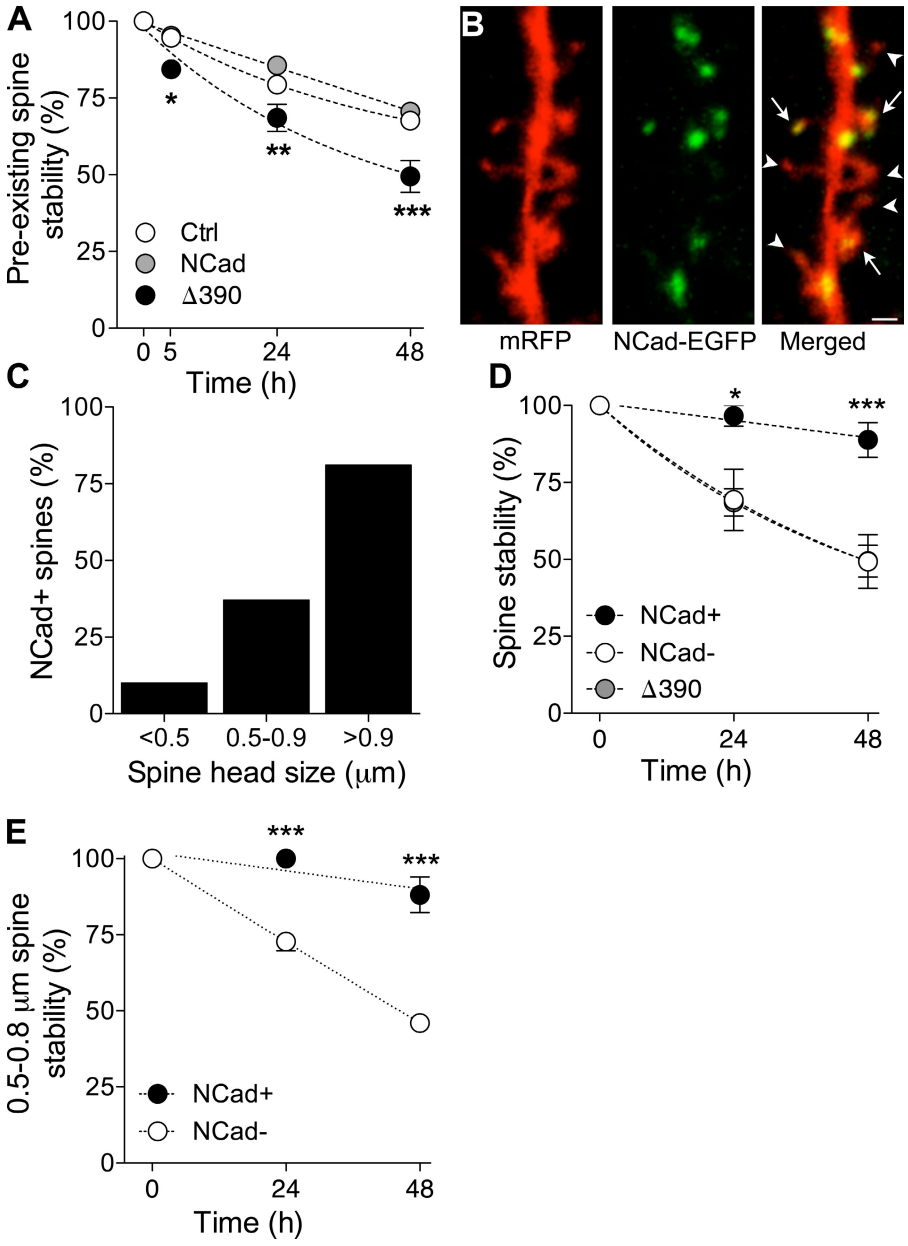

Figure 5. **NCad expression promotes long-term spine stability.** (A) Stability of preexisting spines assessed as the proportion of spine still present on the next 2 d. Data are mean ± SEM of 17, 11, and 9 experiments performed in cells transfected with EGFP (Ctrl), EGFP + NCad (NCad), or EGFP + Δ390-NCad (Δ390; 547, 349, and 358 spines analyzed; *, $P < 0.05$; **, $P < 0.01$; ***, $P < 0.001$; two-way ANOVA with Bonferroni posttest). (B) Expression of EGFP-tagged NCad in a cell transfected with mRFP. Note that several spines express puncta (arrows), whereas others do not (arrowheads). (C) Proportion of spines expressing NCad-EGFP as a function of the spine head size. Data are the mean of six experiments (125 spines analyzed). (D) Long-term stability of spines as a function of NCad-EGFP expression. For comparison, the graph also shows the stability of spines in Δ390-NCad–transfected cells. Data are mean ± SEM of six experiments (125 spines analyzed; *, $P < 0.01$; ***, $P < 0.001$; two-way ANOVA with Bonferroni posttest). (E) Long-term stability as a function of NCad-EGFP expression for spines of sizes between 0.5 and 0.8 µm. Data are mean ± SEM of six experiments (58 spines analyzed; ***, $P < 0.001$; two-way ANOVA with Bonferroni posttest). Bar, 1 µm.

by measuring the probability to remain present on subsequent days. As indicated in Fig. 5 D, spines expressing NCad-EGFP showed a much higher stability than spines devoid of NCad-EGFP ($n = 6$; 125 spines; *, $P < 0.05$; ***, $P < 0.001$; two-way ANOVA). Furthermore, the stability of spines devoid of NCad-EGFP puncta was comparable with the stability of spines in cells expressing mutant Δ390-NCad–EGFP. However, as stability could be linked to both size and NCad-EGFP expression, we selected a group of spines of the same size (0.5–0.8 µm in diameter) and analyzed whether those expressing NCad were also more stable. Fig. 5 E shows the stability over 48 h of 17 spines expressing WT-NCad–EGFP and 41 spines devoid of NCad-EGFP puncta (mean size: 0.66 ± 0.2 µm and 0.63 ± 0.1 µm in diameter, respectively; $P > 0.05$). As illustrated, spines of the same size were still considerably more stable if they expressed NCad puncta ($P < 0.001$; $n = 6$ experiments). Thus, NCad expression directly correlates with long-term spine stability.

NCad is selectively expressed in spines activated by theta burst stimulation

We then investigated whether NCad could contribute to mechanisms of plasticity-induced long-term spine stabilization, and for this, we first examined how activity regulated its expression. We cotransfected pyramidal neurons with mRFP and WT-NCad–EGFP and assessed the proportion of spines exhibiting NCad-EGFP puncta 2–4 d later when exposed to different activity protocols. These experiments were performed in slices maintained under control conditions, or exposed for 60 min to 10 µM carbachol, which induces spontaneous theta activity in the slices (De Roo et al., 2008b), or in slices that received trains of theta burst stimulation. As shown in Fig. S3, the proportion of spines expressing NCad-EGFP puncta was markedly increased after carbachol exposure ($n = 5$; 298 spines analyzed; $P < 0.05$; *t* test) as well as after LTP induction ($n = 6$; 226 spines analyzed; $P < 0.01$; *t* test), whereas

absence of activity did not significantly modify the number of NCad-EGFP–positive spines over 24 h. This effect was selective as it could be prevented by D-AP5 applied during carbachol treatment (n = 4; 190 spines analyzed; $P > 0.05$, t test). Thus, these results suggested that activity selectively targeted NCad at synapses.

To examine this more specifically, we cotransfected CA1 pyramidal neurons with mRFP and NCad-EGFP and then loaded the cell with Fluo4-AM, a calcium indicator, which was applied by bolus loading through an extracellular electrode placed in the vicinity of the transfected cell. At the time of loading (24–48 h after transfection), the green fluorescence of NCad-EGFP was scarce, allowing us to record stimulation-induced calcium signals in spines identified by the red fluorescent dye mRFP (De Roo et al., 2008b). Fig. 6 illustrates one such experiment in which a dendritic segment of an mRFP-transfected CA1 cell (Fig. 6 A) was analyzed at the beginning of the experiments to determine which spines responded to electrical stimulation of a group of CA3 neurons through an extracellular stimulating electrode. This was performed through a line scan analysis of identified spine present on that dendritic segment (Fig. 6 B). The same dendritic segment was then imaged again 5, 24, 48, and 72 h later to determine the long-term stability of each spine (Fig. 6 C). For two specific spines identified on Fig. 6 C with an asterisk and a diamond, we show in Fig. 6 D the green fluorescence calcium signal recorded in the spine. The normalized variations in fluorescence intensity ($\Delta F/F_0$) are illustrated on the right with arrows pointing to the time when a stimulation pulse was applied to a group of CA3 neurons (Fig. 6 D). As illustrated, the spine labeled with an asterisk clearly responded to stimulation with a transient increase in fluorescent intensity, whereas the spine identified by a diamond remained silent (Fig. 6 D). In all experiments, we verified that activated and nonactivated spines were present on the same dendritic segments so as to exclude contamination by dendritic calcium spikes. On average, in three experiments, 45% of tested spines responded to electrical stimulation with the pulse intensities used. Once activated and nonactivated spines were identified, theta burst stimulation was applied through the same electrode using the same stimulation pulses, and the expression of WT-NCad–EGFP was determined in activated and nonactivated spines on subsequent days. Fig. 6 E shows the green fluorescence of NCad-EGFP puncta observed 24 h after theta burst stimulation on the same dendritic segment illustrated in Fig. 6 C. As shown in Fig. S3, theta burst stimulation triggered a significant increase in the appearance of identifiable puncta. In three experiments, 31 activated and 29 nonactivated spines could be analyzed, of which 31 expressed NCad-EGFP puncta 24 h after theta burst stimulation. Analysis of the localization of NCad-EGFP puncta revealed that 21 out of 31 activated spines expressed NCad-EGFP puncta, whereas only 10 out of 29 nonstimulated spines did (Fig. 6 F). Furthermore, 68% of newly formed NCad-EGFP puncta appeared in activated spines, but only 32% of them appeared in nonactivated spines (Fig. 6 G). Thus, formation of NCad-EGFP puncta preferentially occurred in spines stimulated with theta burst activity.

NCad function is required for plasticity-induced long-term spine stabilization

We then examined whether activity-dependent expression of NCad could account for the structural remodeling and the stabilization of stimulated synapses after induction of synaptic plasticity. Induction of LTP has been shown to result in an enlargement of the spine head and a selective, long-term stabilization of activated synapses (Matsuzaki et al., 2004; De Roo et al., 2008b). For these experiments, CA1 pyramidal neurons were cotransfected with mRFP and either NCad or Δ390-NCad and then loaded 2 d later with Fluo4-AM to determine, as illustrated in Fig. 6, which spines on a dendritic segment responded by a calcium signal to electrical stimulation of a group of CA3 neurons. These synapses were then activated with theta burst stimulation using the same stimulation conditions, and the changes in size of activated and nonactivated spines were determined as well as their long-term stability. As shown in Fig. 6 H, although most activated synapses in mRFP-transfected cells showed an enlargement of their spine head 5 h later (n = 4; 16 activated and 63 nonactivated spines analyzed; $P < 0.05$), this was neither observed in WT-NCad– nor in Δ390-NCad–transfected neurons (n = 6 and 5; 122–168 synapses analyzed). Thus, this result suggests that unaltered endogenous NCad function is required for spine enlargement. More importantly, Fig. 6 (I and J) shows that the long-term stabilization of activated synapses recently described after LTP induction (De Roo et al., 2008b) still occurred in NCad-transfected neurons (n = 8; 114 activated and 90 nonactivated spines analyzed; $P < 0.001$; two-way ANOVA) but was fully prevented in Δ390-NCad–expressing cells (n = 5; 55 activated and 67 nonactivated spines analyzed; $P > 0.05$; two-way ANOVA). Thus, NCad function plays a critical role in the long-term plasticity-induced stabilization of excitatory synapses.

To further determine the role of NCad in plasticity-mediated stabilization of spines, we also examined the correlation between expression of NCad-EGFP and long-term stability in stimulated synapses, as determined by calcium imaging experiments. Out of 31 stimulated spines analyzed in three separate experiments, 21 expressed NCad-EGFP puncta 24 h later and 10 did not. By analyzing the stability of these stimulated synapses over 48 h, we find that 90% of those that expressed NCad-EGFP were still present (19 out of 21 spines), whereas only 60% of those that did not express NCad-EGFP survived (6 out of 10 spines; $P < 0.05$; χ^2 test; Fig. S4). For comparison, analysis of the stability of nonstimulated spines that did not express NCad-EGFP showed that their probability to persist for 48 h was only 49 ± 8% (Fig. 5 D). Thus, plasticity-induced expression of NCad plays a key role in promoting the long-term persistence of stimulated synapses.

Finally, to confirm in a different manner the results obtained by overexpression of a dominant-negative mutant NCad, we also performed experiments using a short hairpin RNA (shRNA) approach to down-regulated NCad. Neurons were transfected with either a commercially available anti-NCad shRNA (shNCad) or a control, scrambled shRNA (shCtrl). Down-regulation of NCad resulted in a very similar phenotype as overexpression of mutant NCad. As illustrated in Fig. 7, cells

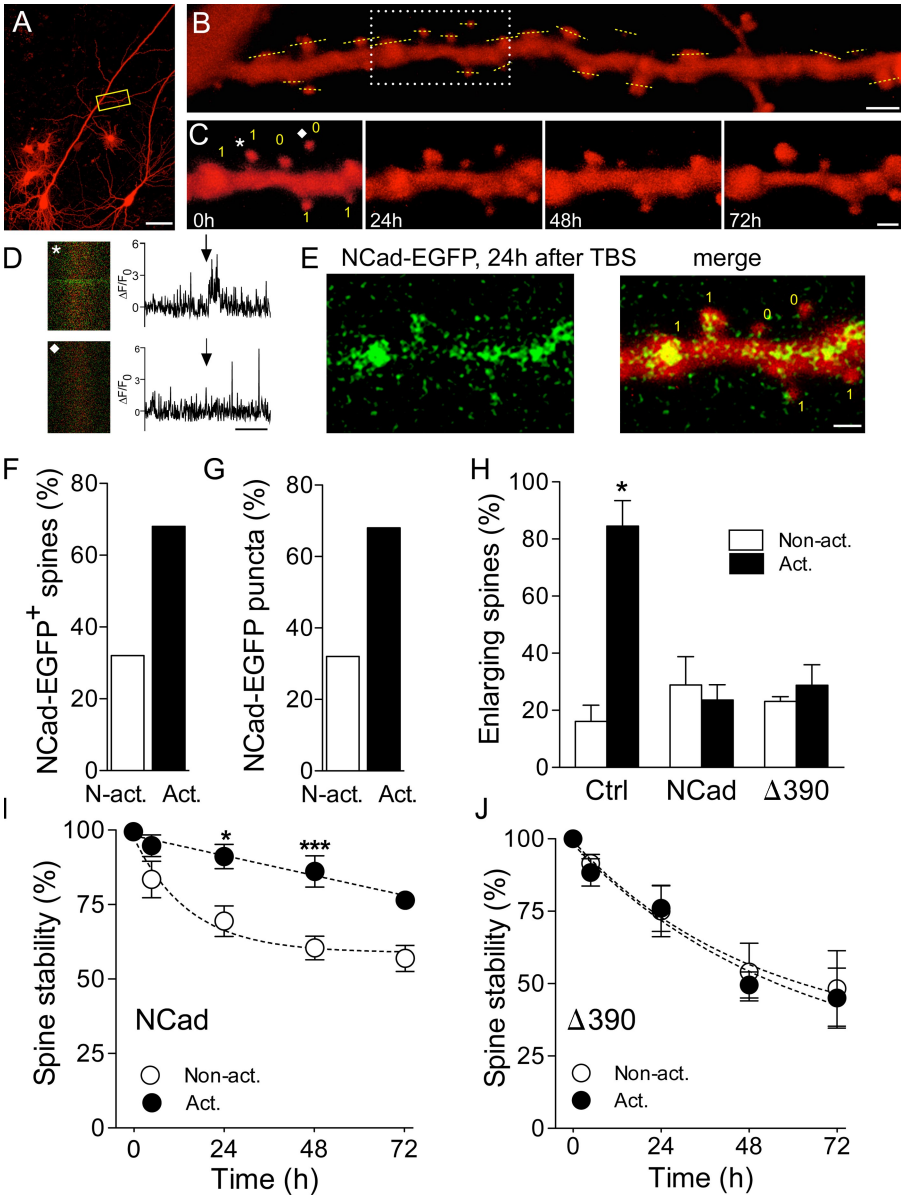

Figure 6. **NCad is selectively expressed in potentiated synapses and is required for their long-term stabilization.** (A) Illustration of an mRFP-transfected pyramidal neuron with the localization of a dendritic segment analyzed in B and C. The box shows the dendritic segment enlarged in B. (B) The mRFP-transfected cell in A was loaded with Fluo4-AM through bolus loading, and spines were tested using line scans (yellow dashed lines) for their response to stimulation pulses applied in the CA3 area. The delimited region shows the portion of dendrite illustrated in C. (C) Repetitive imaging at 24-h intervals of the same dendritic segment. The yellow number indicate whether the spines were activated (1) or not (0) by the stimulation pulses applied to CA3 neurons. The asterisk and the diamond show the localization of the spines in which the calcium signals illustrated in D were recorded. (D) Line scans obtained in the spines indicated by an asterisk or diamond in C. The graph shows the $\Delta F/F_0$ values for the corresponding line scans. Arrows indicate stimulation. (E) NCad-EGFP fluorescence (left) and signal merged with the mRFP fluorescence (merge) observed on the same dendritic segment 24 h after theta burst stimulation (TBS). Note that no NCad-EGFP fluorescence was detectable at time 0 (not depicted). The yellow numbers indicate which spines were activated (1) or not (0) by theta burst stimulation. (F) Proportion of activated (act.) and nonactivated (N-act.) spines expressing NCad-EGFP 24 h after theta burst stimulation (n = 31 activated and 29 nonactivated spines out of three experiments). (G) Proportion of NCad-EGFP puncta that appeared in activated versus nonactivated spines (n = 29 new puncta in three experiments). (H) Proportion of activated and nonactivated spines (mean ± SEM) that showed an enlargement of their spine head 5 h after theta burst stimulation (n = 4–6 experiments; 79, 168, and 122 spines analyzed in control [Ctrl]-, NCad-, and Δ390-NCad–transfected cells; *, $P < 0.05$; t test). (I) Stability of activated and nonactivated spines analyzed as the proportion of them still present on consecutive days in cells transfected with WT-NCad. Data are mean ± SEM of eight experiments (114 activated and 90 nonactivated spines analyzed; *, $P < 0.05$; ***, $P < 0.001$; two-way ANOVA with Bonferroni posttest). (J) Same as in I but for cells transfected with Δ390-NCad (n = 5; 55 activated and 67 nonactivated spines analyzed; $P > 0.05$; two-way ANOVA with Bonferroni posttest). Bars: (A) 100 µm; (B) 2 µm; (C and E) 1 µm; (D) 1 s.

transfected with shNCad exhibited smaller dendritic spines than cell transfected with shCtrl, the effect being characterized by a shift to the left of the spine head width distribution (mean spine head diameter: 0.54 ± 0.03 µm vs. 0.70 ± 0.04 µm; n = 191 and 172, respectively; $P < 0.01$). Additionally, the general stability of spines was reduced in cells transfected with shNCad versus shCtrl (n = 7 and 6 cells; *, $P < 0.05$; two-way ANOVA with Bonferroni posttest; Fig. 7 B). Finally, we also analyzed the capacity to promote long-term stabilization of activated spines through LTP induction. As shown in Fig. 7 (C and D), induction of plasticity through theta bust stimulation resulted in a specific long-term stabilization of activated spines in shCtrl-transfected cells (n = 3; 43 activated and 36 nonactivated spines analyzed; ***, $P < 0.001$; two-way ANOVA with Bonferroni posttest), as observed in Fig. 6, but failed completely to stabilize activated spines in shNCad-transfected neurons (n = 4; 41 activated and 45 nonactivated spines analyzed). Thus, this result confirms the critical role played by NCad in promoting a plasticity-mediated long-term stabilization of dendritic spines.

Discussion

By examining the long-term behavior of spines in relationship to activity and NCad expression, this study provides the first direct evidence that NCad, when expressed through activity and induction of plasticity, is able to switch stimulated synapses to

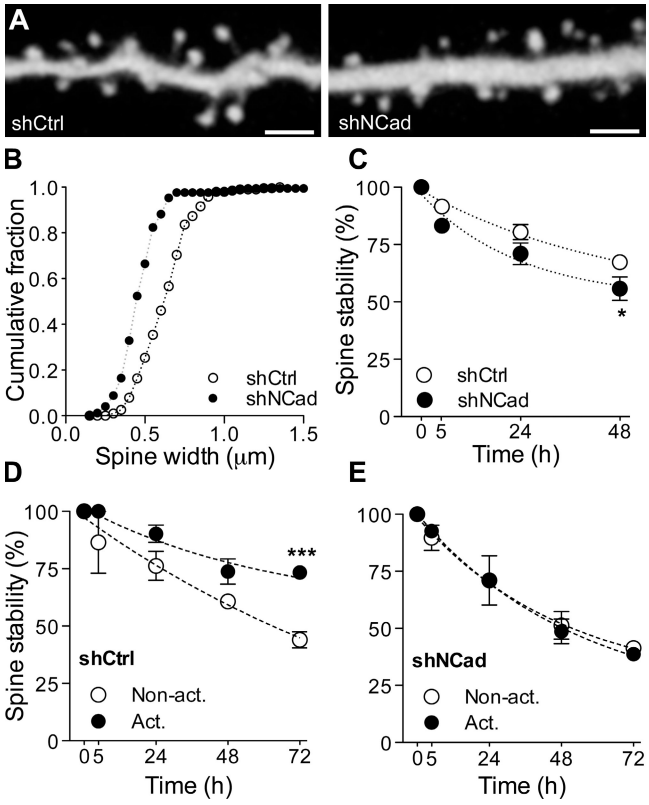

Figure 7. **Knockdown of NCad interferes with plasticity-induced spine stabilization.** (A) Illustration of dendritic segments of pyramidal neurons cotransfected with mRFP and either control shRNA (left) or shRNA against NCad (right). (B) Expression of an shRNA against NCad (shNCad; $n = 7$ cells) results in a decrease in spine head width when compared with expression of a control shRNA (shCtrl; $n = 6$ cells). (C) The stability of spines of cells transfected with shNCad ($n = 4$) was reduced as compared with cells transfected with shCtrl ($n = 7$; mean ± SEM; *, $P < 0.05$; two-way ANOVA with Bonferroni posttest). (D) LTP induces an increased stabilization of activated spines (Act.) versus nonactivated spines (Non-act.) in cells transfected with shCtrl. Data are mean ± SEM of three experiments (79 spines analyzed; ***, $P < 0.001$; two-way ANOVA with Bonferroni posttest). (E) In contrast, LTP did not promote a selective stabilization of activated spines versus nonactivated ones in cells transfected with shNCad ($n = 4$; 86 spines analyzed; mean ± SEM). Bars, 2 μm.

a highly stable state. Therefore, NCad functions as a molecular marker or tag of persistent synapses. A causal link between synaptic expression of NCad and long-term stability is supported by several key observations.

First, in agreement with much previous work that analyzed the role of NCad function and signaling in spine morphogenesis (Togashi et al., 2002; Abe et al., 2004; Xie et al., 2008; Arikkath et al., 2009), we also find that NCad controls the size of the spine, a parameter directly linked to spine and synapse stability (Harris et al., 1992; Trachtenberg et al., 2002; Holtmaat et al., 2005; for review see Kasai et al., 2003). Interestingly, this effect was associated with modifications of the PSD. Upon expression of NCad, spines enlarged but also expressed larger PSDs and larger PSD-95 puncta, whereas, conversely, interference with NCad function led to thin, filopodia-like spines, still making synapses but with small PSDs. This was further confirmed by analyzing newly formed spines in which NCad also promoted PSD-95 expression. Thus, in addition to regulating spine size, probably through Rho GTPases and the cytoskeleton (Xie et al., 2008), NCad also controls the expression of PSD-95 and the organization of the PSD.

However, the most compelling evidence for a role of NCad in spine stability is provided by the direct assessment of spine behavior through repetitive imaging. Both newly formed spines and preexisting spines of a neuron were markedly destabilized by mutant NCad and by suppression of NCad expression. More significantly, spines that expressed NCad were selectively more stable than spines on the same neuron devoid of NCad. Thus, long-term spine stability directly correlates with NCad expression.

Interestingly, spines that expressed NCad also tended to be larger, thus raising the issue of the relationship between stability and changes in spine size, NCad being important for both parameters (Matsuzaki et al., 2004; Yasumatsu et al., 2008). We found that even if we compare spines of the same range of sizes, those that expressed NCad were significantly more stable, indicating that the adhesion molecule has a direct effect on stability independently of the absolute size. Thus, NCad expression probably affects size and stability through distinct mechanisms, but in a very correlated manner. Consistent with this idea, expression of WT-NCad prevented LTP-induced enlargement of stimulated spines but not their stabilization.

Another question regards the conditions under which NCad becomes expressed at synapses. As shown by the experiments with tagged NCad, not all spines do express detectable NCad puncta, which is a result very different from that obtained with tagged PSD-95. Interestingly, by exploiting the activity dependency of the cytomegalovirus promoter, we could enhance the expression of tagged NCad by stimulating neurons with theta burst activity during the first days after transfection. This property allowed us to trigger expression and then examine where NCad became expressed. The results clearly revealed that NCad puncta preferentially appear at stimulated synapses and thus that NCad is selectively targeted to stimulated spines. This effect was NMDA receptor dependent and therefore suggests that NCad functions as a kind of molecular tag of potentiated synapses, as recently proposed for Homer-1a (Okada et al., 2009). This is also in agreement with previous data showing that activity and NMDA receptors regulate NCad expression at synapses in dissociated cultures (Bozdagi et al., 2000; Tai et al., 2007; Arikkath et al., 2009). Together, these experiments suggest that one key aspect of LTP mechanisms could be the expression of NCad to provide long-term stability to the synapse (De Roo et al., 2008b). As shown in this study, interference with NCad function, either through expression of mutant NCad or through shRNA down-regulation, fully prevented the LTP-mediated stabilization of stimulated spines. Conversely, the stability of spines expressing NCad or a control shRNA was very much similar to that of spines stabilized through induction of LTP. Thus, these experiments provide the first direct evidence for a link between induction of plasticity, expression of a specific molecule, and synapse persistence. However, it should be noted that NCad is possibly not the only molecule contributing to spine persistence. A role for other adhesion molecules or PSD proteins cannot be excluded by these experiments.

The role of NCad in spine stability could also explain other aspects of the morphological changes observed upon interference with the function of the molecule. The increased spine turnover observed with mutant NCad or catenins (Abe et al., 2004) could reflect difficulties to stabilize synapses and the promotion of compensatory mechanisms to maintain synapse number and activity level.

Finally, a last question concerns the mechanisms through which NCad confers long-term stability to synapses. Although this could be linked to the signaling of NCad through Rho GTPases and the cytoskeleton (Xie et al., 2008), another likely possibility could be that stability comes from the strong adhesion that the molecule provides across the synapse (Tanaka et al., 2000). The existence of organized periodic complexes across the synaptic cleft compatible with a zipper organization of NCad has been proposed (Zuber et al., 2005). This could anchor pre- and postsynaptic membranes together so as to stabilize the organization and growth of the PSD.

In conclusion, these experiments provide the first strong evidence that NCad represents a key molecule regulating long-term synapse stability and that its enhanced expression during synaptic plasticity is required for the structural remodeling of the synapse and its persistence. By maintaining functionally important synapses, NCad could work as a memory molecule allowing the persistence of synaptic contacts selected through plasticity and thus ensure the specificity of synaptic networks.

Materials and methods

Cultures and transfections

Transverse hippocampal organotypic slice cultures (400 µm thick) were prepared from 6–7-d-old rats using a protocol approved by the Geneva Veterinarian Office (authorization 31.1.1007/3129/0) and maintained for 15 d in culture as described previously (Stoppini et al., 1991). To facilitate transfer of slice cultures to recording conditions, they were cultured on a small membrane confetti (6–8 mm in diameter; Millipore) placed on top of the Millipore insert. For the visualization of spines, slice cultures were transfected using a biolistic method (Helios Gene Gun; Bio-Rad Laboratories) 2–4 d before the first observation, which occurred at day in vitro 11. The number of transfected CA1 pyramidal cells varied between zero and five per slice culture; fluorescence usually started to be expressed after 24–48 h. The plasmid DNAs were precipitated onto 10 mg of 1.6-µm gold microcarriers using a threefold excess for nonfluorescent proteins. Control experiments showed that cells cotransfected with EGFP and DsRed constructs (1:3 ratio) expressed green and red fluorescence in most cases. pcDNA3 was used as the vector for expression of EGFP and the myc-tagged WT and mutated forms of mouse NCad. These constructs as well as PSD-95–DsRed2 were expressed under the control of the cytomegalovirus promoter. Myc-tagged WT and mutated forms of mouse NCad were provided by R.L. Huganir (Johns Hopkins School of Medicine, Baltimore, MD). The expression vector for PSD-95 fused at its C terminus with EGFP was a gift from D.S. Bredt (University of California, San Francisco, San Francisco, CA). PSD-95–DsRed2 fusion was constructed by introducing PSD-95 cDNA in the pDsRed-N1 vector (Takara Bio Inc.). Mutated and WT-NCad were fused to the N-terminal amino acid of EGFP using the pEGFPN1 vector (Takara Bio Inc.). mRFP (a gift from A.K. Hadjantonakis and R.Y. Tsien, University of California, San Diego, La Jolla, CA) was transfected using a pCX-mRFP1 plasmid under the control of the chicken β-actin promoter. We used a commercially available shRNA against NCad (Mission shRNA; Sigma-Aldrich) directed against the NCad sequence 5′-GCAGGCAAAGTTCCTGATATA-3′.

Confocal imaging and analysis

Laser-scanning microscopy was realized with a Fluoview 300 system (Olympus) using a 488-nm argon laser and a 537-nm helium-neon laser or a 2-photon laser set at 920 nm (Coherent). The experiments with PSD-95–DsRed2-transfected slices were collected using a spinning-disk confocal system (Visitron) and two excitation lasers set at 488 and 568 nm. Repetitive confocal imaging experiments were performed as described previously (De Roo et al., 2008a). In brief, transfected slice cultures were maintained in a recording chamber at room temperature under immersion conditions with culture serum for the time of observation and then transferred back to the incubator. An image of the entire CA1 pyramidal neuron with steps of 3 µm between scans was performed the first and last imaging day using a 40× 0.80 NA objective (Olympus) to check for the general morphology and health of the selected neuron. All analyses were performed on dendritic segments of ∼35 µm in length and located between 100 and 200 µm from the soma (one segment per cell and per experiment) and imaged with a 40× objective using a 8–10× additional zoom (final definition, 20–25 pixels/µm; steps between scans, 0.25–0.5 µm).

Analyses of spine turnover and survival were performed blind on z stacks of raw images using a plugin specifically developed for OsiriX software (http://www.osirix-viewer.com). Protrusions were classified as filopodia-like protrusions (protrusions without enlargement at the tip) or spines (protrusions with a neck and an enlargement at the tip). Head width was measured as the biggest diameter of the head. Maximal intensity projections of the z stacks were used to analyze the presence or absence of PSD-95–DsRed2 or NCad-EGFP puncta in neurons cotransfected with EGFP or mRFP, respectively. The mean intensity was measured in the red channel for PSD-95–DsRed2 or in the green channel for NCad-EGFP in regions of interest corresponding to the spine heads observed in the green or red channel, respectively. Mean intensity values were compared with background determined in neighboring spine head or dendrites with no detectable puncta. Spines were considered positive for PSD-95–DsRed2 or NCad-EGFP staining if this mean intensity was more than two times higher than the background determined in neighboring spine head or dendrite parts with no detectable puncta. The minimal mean intensity measured for a positive spine was 2.1 times the background, and the maximal was 5.1 times the background. For PSD-95 cluster analysis, maximum intensity z projections of stacks were used. Cluster size was determined by measuring the maximal diameter of puncta. Only clusters bigger than 0.3 µm in maximal diameter and at least twice as bright as the dendritic shaft were measured. The ensemble of the dataset for cluster size followed a Gaussian distribution, indicating no systematic bias introduced by the criteria.

For calcium imaging of spine activity, cells were transfected with both mRFP and NCad-EGFP. Because of the use of different promoters, expression of mRFP was clearly faster (1–2 d) than expression of NCad-EGFP (2–4 d). After 2 d, cells that expressed mRFP but not yet NCad-EGFP were selected and loaded (one cell per culture) with the cell-permeable calcium indicator Fluo4-AM (F-14201; Invitrogen). For this, 50 µg Fluo4-AM was dissolved in 10 µl Pluronic (F-127; Invitrogen) and then diluted in 90 µl of standard pipette solution (150 mM NaCl, 2.5 mM KCl, and 10 mM Hepes) for a final dye concentration of 500 µM. A standard patch pipette was then filled with 10 µl of dye solution and placed at a distance of ∼10 µm from the soma. Dye was ejected by short pulses of pressured air at a frequency of three per minute during 0.5 h. Calcium transients were then recorded using line scans (Fluoview 300; 40× objective; Olympus) through the spine heads obtained during application of stimulation pulses to Schaffer collaterals. Stimulating electrode was always placed at minimum at 500 µm from the dendritic tree of the Fluo4-AM–loaded cell to preclude direct electrical stimulation of the cell. In all experiments performed, we also verified that spines activated by stimulation were always surrounded by other silent, nonactivated spines to exclude global activation effects. Spines located too close to each other were excluded from analysis. Confocal aperture was set to the minimum during line scans, and matching with the mRFP fluorescence in the red channel was systematically checked. For each spine tested, three to seven line scans of 8-s duration were performed, with an electrical stimulation pulse occurring automatically at 3 s. Calcium responses were measured as $\Delta F/F_0$, where F_0 is the mean fluorescence measured during the baseline. Detection of NCad-EGFP puncta in stimulated and nonstimulated spines was performed 24 h later. As described in the previous paragraph, spines were considered positive if the mean intensity was no more than two times higher than the background determined in neighboring spine head or dendrite parts with no detectable puncta.

All statistics are given with the SEM. Standard *t* tests were performed to compare Gaussian distributions, and Mann-Whitney tests were used for non-Gaussian distributions. For all tests, α was set to 5%.

EM

After confocal imaging of transfected cells, slice cultures were fixed with 2% paraformaldehyde and 0.2% glutaraldehyde in 0.1 M of phosphate

buffer, pH 7.4, cryoprotected, freeze-thawed in liquid nitrogen, and incubated overnight in primary antibody (1:500 rabbit anti-GFP; Millipore) at 4°C and then in biotinylated secondary antibody (1:200 goat anti-rabbit; Fab Fragment; Jackson ImmunoResearch Laboratories, Inc.) and in avidin biotin peroxidase complex (ABC Elite; Vector Laboratories) followed by 3,3′-diaminobenzidine tetrachloride and 0.015% hydrogen peroxide. After embedding in Epon resin (Fluka), the cultures were trimmed for cutting around labeled cells of interest, and serial ultrathin sections (60 nm) were cut. Images of labeled dendrites from the middle portion of CA1 stratum radiatum were taken at a magnification of 9,700–15,000 using transmission electron microscopes (Philips CM10, Philips CM12, and Tecnai G212; FEI Company) equipped with digital cameras (Mega View III and Morada; Soft Imaging Systems). Synapses were defined by the presence of a PSD facing at least two to three presynaptic vesicles. Complex or perforated PSDs were defined by the presence of a discontinuity on a single section. Terminals were identified by the presence of an enlargement of the axonal shaft containing vesicles and facing at least one PSD. Digital serial electron micrographs were aligned using Photoshop software (Adobe). 3D reconstructions as well as surface, volume, and length measurements were performed using Neurolucida software (version 6.02; MicroBrightField, Inc). 3D illustrations were made using software Reconstruct developed by J.C. Fiala and K.M. Harris (Synapse Web, http://synapse-web.org/tools/reconstruct/reconstruct.stm) followed by color rendering with 3D Studio Max (Discreet Software).

Online supplemental material

Fig. S1 shows that loss of function of NCad results in increased formation of filopodia-like protrusions. Fig. S2 shows that new spine stabilization induced by blockade of AMPA receptors with NBQX is prevented by mutant Δ390-NCad expression. Fig. S3 shows that activity promotes expression of NCad puncta in spines. Fig. S4 shows that plasticity-mediated expression of NCad correlates with long-term persistence of spines. Online supplemental material is available at http://www.jcb.org/cgi/content/full/jcb.201003007/DC1.

We thank Marlis Moosmayer, Lorena Jourdain, Irina Nikonenko, and Philippe Corrèges for technical support and Joël Spaltenstein for the developments of OsiriX software plugins. The mRFP1 plasmid was a gift from A.K. Hadjantonakis and R.Y. Tsien.

This work was supported by the Swiss National Science Foundation, Boninchi Foundation, Velux Foundation, and European project Promemoria.

Submitted: 1 March 2010
Accepted: 13 April 2010

References

Abe, K., O. Chisaka, F. Van Roy, and M. Takeichi. 2004. Stability of dendritic spines and synaptic contacts is controlled by alpha N-catenin. *Nat. Neurosci.* 7:357–363. doi:10.1038/nn1212

Arikkath, J., and L.F. Reichardt. 2008. Cadherins and catenins at synapses: roles in synaptogenesis and synaptic plasticity. *Trends Neurosci.* 31:487–494. doi:10.1016/j.tins.2008.07.001

Arikkath, J., I.F. Peng, Y.G. Ng, I. Israely, X. Liu, E.M. Ullian, and L.F. Reichardt. 2009. Delta-catenin regulates spine and synapse morphogenesis and function in hippocampal neurons during development. *J. Neurosci.* 29:5435–5442. doi:10.1523/JNEUROSCI.0835-09.2009

Bozdagi, O., W. Shan, H. Tanaka, D.L. Benson, and G.W. Huntley. 2000. Increasing numbers of synaptic puncta during late-phase LTP: N-cadherin is synthesized, recruited to synaptic sites, and required for potentiation. *Neuron*. 28:245–259. doi:10.1016/S0896-6273(00)00100-8

De Roo, M., P. Klauser, P. Mendez, L. Poglia, and D. Muller. 2008a. Activity-dependent PSD formation and stabilization of newly formed spines in hippocampal slice cultures. *Cereb. Cortex*. 18:151–161. doi:10.1093/cercor/bhm041

De Roo, M., P. Klauser, and D. Muller. 2008b. LTP promotes a selective long-term stabilization and clustering of dendritic spines. *PLoS Biol.* 6:e219. doi:10.1371/journal.pbio.0060219

Elia, L.P., M. Yamamoto, K. Zang, and L.F. Reichardt. 2006. p120 catenin regulates dendritic spine and synapse development through Rho-family GTPases and cadherins. *Neuron*. 51:43–56. doi:10.1016/j.neuron.2006.05.018

Grutzendler, J., N. Kasthuri, and W.B. Gan. 2002. Long-term dendritic spine stability in the adult cortex. *Nature*. 420:812–816. doi:10.1038/nature01276

Harris, K.M., F.E. Jensen, and B. Tsao. 1992. Three-dimensional structure of dendritic spines and synapses in rat hippocampus (CA1) at postnatal day 15 and adult ages: implications for the maturation of synaptic physiology and long-term potentiation. *J. Neurosci.* 12:2685–2705.

Harvey, C.D., and K. Svoboda. 2007. Locally dynamic synaptic learning rules in pyramidal neuron dendrites. *Nature*. 450:1195–1200. doi:10.1038/nature06416

Holtmaat, A.J., J.T. Trachtenberg, L. Wilbrecht, G.M. Shepherd, X. Zhang, G.W. Knott, and K. Svoboda. 2005. Transient and persistent dendritic spines in the neocortex in vivo. *Neuron*. 45:279–291. doi:10.1016/j.neuron.2005.01.003

Honkura, N., M. Matsuzaki, J. Noguchi, G.C. Ellis-Davies, and H. Kasai. 2008. The subspine organization of actin fibers regulates the structure and plasticity of dendritic spines. *Neuron*. 57:719–729. doi:10.1016/j.neuron.2008.01.013

Kasai, H., M. Matsuzaki, J. Noguchi, N. Yasumatsu, and H. Nakahara. 2003. Structure-stability-function relationships of dendritic spines. *Trends Neurosci.* 26:360–368. doi:10.1016/S0166-2236(03)00162-0

Kopec, C.D., E. Real, H.W. Kessels, and R. Malinow. 2007. GluR1 links structural and functional plasticity at excitatory synapses. *J. Neurosci.* 27:13706–13718. doi:10.1523/JNEUROSCI.3503-07.2007

Lendvai, B., E.A. Stern, B. Chen, and K. Svoboda. 2000. Experience-dependent plasticity of dendritic spines in the developing rat barrel cortex in vivo. *Nature*. 404:876–881. doi:10.1038/35009107

Matsuzaki, M., N. Honkura, G.C. Ellis-Davies, and H. Kasai. 2004. Structural basis of long-term potentiation in single dendritic spines. *Nature*. 429:761–766. doi:10.1038/nature02617

Okada, D., F. Ozawa, and K. Inokuchi. 2009. Input-specific spine entry of soma-derived Vesl-1S protein conforms to synaptic tagging. *Science*. 324:904–909. doi:10.1126/science.1171498

Okamura, K., H. Tanaka, Y. Yagita, Y. Saeki, A. Taguchi, Y. Hiraoka, L.H. Zeng, D.R. Colman, and N. Miki. 2004. Cadherin activity is required for activity-induced spine remodeling. *J. Cell Biol.* 167:961–972. doi:10.1083/jcb.200406030

Okuda, T., L.M. Yu, L.A. Cingolani, R. Kemler, and Y. Goda. 2007. beta-Catenin regulates excitatory postsynaptic strength at hippocampal synapses. *Proc. Natl. Acad. Sci. USA*. 104:13479–13484. doi:10.1073/pnas.0702334104

Saglietti, L., C. Dequidt, K. Kamieniarz, M.C. Rousset, P. Valnegri, O. Thoumine, F. Beretta, L. Fagni, D. Choquet, C. Sala, et al. 2007. Extracellular interactions between GluR2 and N-cadherin in spine regulation. *Neuron*. 54:461–477. doi:10.1016/j.neuron.2007.04.012

Steiner, P., M.J. Higley, W. Xu, B.L. Czervionke, R.C. Malenka, and B.L. Sabatini. 2008. Destabilization of the postsynaptic density by PSD-95 serine 73 phosphorylation inhibits spine growth and synaptic plasticity. *Neuron*. 60:788–802. doi:10.1016/j.neuron.2008.10.014

Stoppini, L., P.A. Buchs, and D. Muller. 1991. A simple method for organotypic cultures of nervous tissue. *J. Neurosci. Methods*. 37:173–182. doi:10.1016/0165-0270(91)90128-M

Tai, C.Y., S.P. Mysore, C. Chiu, and E.M. Schuman. 2007. Activity-regulated N-cadherin endocytosis. *Neuron*. 54:771–785. doi:10.1016/j.neuron.2007.05.013

Tanaka, H., W. Shan, G.R. Phillips, K. Arndt, O. Bozdagi, L. Shapiro, G.W. Huntley, D.L. Benson, and D.R. Colman. 2000. Molecular modification of N-cadherin in response to synaptic activity. *Neuron*. 25:93–107. doi:10.1016/S0896-6273(00)80874-0

Tanaka, J., Y. Horiike, M. Matsuzaki, T. Miyazaki, G.C. Ellis-Davies, and H. Kasai. 2008. Protein synthesis and neurotrophin-dependent structural plasticity of single dendritic spines. *Science*. 319:1683–1687. doi:10.1126/science.1152864

Tang, L., C.P. Hung, and E.M. Schuman. 1998. A role for the cadherin family of cell adhesion molecules in hippocampal long-term potentiation. *Neuron*. 20:1165–1175. doi:10.1016/S0896-6273(00)80497-3

Togashi, H., K. Abe, A. Mizoguchi, K. Takaoka, O. Chisaka, and M. Takeichi. 2002. Cadherin regulates dendritic spine morphogenesis. *Neuron*. 35:77–89. doi:10.1016/S0896-6273(02)00748-1

Trachtenberg, J.T., B.E. Chen, G.W. Knott, G. Feng, J.R. Sanes, E. Welker, and K. Svoboda. 2002. Long-term in vivo imaging of experience-dependent synaptic plasticity in adult cortex. *Nature*. 420:788–794. doi:10.1038/nature01273

Xie, Z., H. Photowala, M.E. Cahill, D.P. Srivastava, K.M. Woolfrey, C.Y. Shum, R.L. Huganir, and P. Penzes. 2008. Coordination of synaptic adhesion with dendritic spine remodeling by AF-6 and kalirin-7. *J. Neurosci.* 28:6079–6091. doi:10.1523/JNEUROSCI.1170-08.2008

Yasumatsu, N., M. Matsuzaki, T. Miyazaki, J. Noguchi, and H. Kasai. 2008. Principles of long-term dynamics of dendritic spines. *J. Neurosci.* 28:13592–13608. doi:10.1523/JNEUROSCI.0603-08.2008

Zito, K., V. Scheuss, G. Knott, T. Hill, and K. Svoboda. 2009. Rapid functional maturation of nascent dendritic spines. *Neuron*. 61:247–258. doi:10.1016/j.neuron.2008.10.054

Zuber, B., I. Nikonenko, P. Klauser, D. Muller, and J. Dubochet. 2005. The mammalian central nervous synaptic cleft contains a high density of periodically organized complexes. *Proc. Natl. Acad. Sci. USA*. 102:19192–19197. doi:10.1073/pnas.0509527102

Zuo, Y., A. Lin, P. Chang, and W.B. Gan. 2005. Development of long-term dendritic spine stability in diverse regions of cerebral cortex. *Neuron*. 46:181–189. doi:10.1016/j.neuron.2005.04.001